Figure S1. Verification of mono-ADP-ribosylation in Lovo cells using immunofluorescence. Immunofluorescence images showing mono-ADP-ribosylation binding regions (red) and the nucleus (blue). Scale bar, 25 μm.

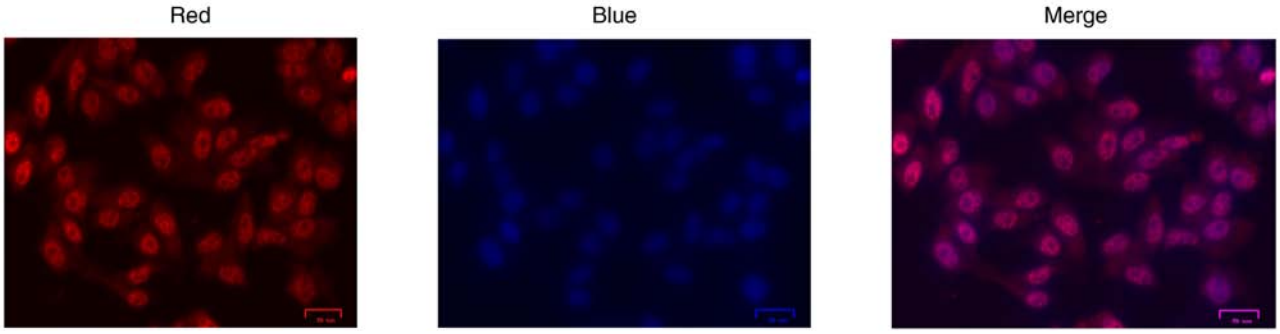

Figure S2. Identification of the glycosaminoglycan biosynthesis-chondroitin sulfate/dermatan sulfate pathway. Relative expression of (A) CHST12, (B) B3GALT6 and (C) CHST15 in the untransfected and transfected cells was assessed using quantitative PCR. Error bars represent the mean ± standard deviation. n=3. $^{**}P<0.01$, $^{***}P<0.0001$ vs. untransfected Lovo cells. CHST12, chondroitin 4-sulfotransferase; B3GALT6, galactosylxylosyl protein 3-β-galactosyltransferase; CHST15, N-acetyl galactosamine 4-sulfate 6-O-sulfotransferase.

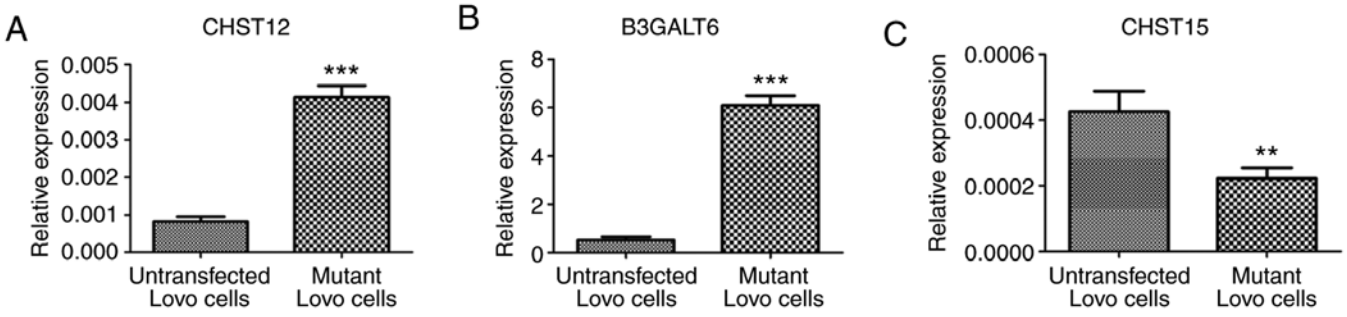

Figure S3. Effect of mono-ADP-ribosylation of H3R117 on invasion and metastasis and on Wnt/β-catenin signaling. (A) The invasive capacity of Lovo cells was evaluated using a Transwell invasion assay. Magnification, x200. Cell counts were performed using ImageJ. (B) The migratory capacity of Lovo cells were evaluated using a wound healing assay. Wounds were imaged at 0 and 24 h. Wound closure was analyzed using ImageJ. Scale bar, 100 μm. (C) Western blotting and (D) immunofluorescence experiments were used to evaluate the protein expression levels. Densitometry analysis was performed using Image Lab, and average optical density was analyzed using ImageJ. Scale bar, 50 μm. Each experiment was repeated three times. Error bars represent the mean ± standard deviation. n=3. *P<0.05, ***P<0.0001 vs. untransfected Lovo cells. H3, histone H3.